Available online at www.sciencedirect.com
SCIENCE DIRECT
Robotics and Autonomous Systems 54 (2006) 574–589
Robotics and Autonomous Systems
www.elsevier.com/locate/robot

Fuzzy potential energy for a map approach to robot navigation☆

Kuo-Yang Tu[a,*], Jacky Baltes[b]

[a] *Institute of Systems and Control Engineering, National Kaohsiung First University of Science and Technology, No. 2, Juoyue Road, Nantsu District, Kaohsiung, 811, Taiwan, ROC*
[b] *Department of Computer Science, University of Manitoba, Canada*

Received 31 January 2005; received in revised form 5 August 2005; accepted 6 April 2006
Available online 26 May 2006

Abstract

A fully autonomous robot needs a flexible map to solve frequent change of robot situations and/or tasks. In this paper, based on the second type of fuzzy modeling, fuzzy potential energy (FPE) is proposed to build a map that facilitates planning robot tasks for real paths. Three rules for making use of FPEs are derived to ground the basic ideas of building a map for task navigation. How the FPE performs robot navigation is explained by its gradient directions and shown by its gradient trajectories. To code qualitative information into quantity, the proposed FPE provides a way to quickly find a path for conducting the designated task or solving a robot under an embarrassing situation. This paper pioneers novel design and application of fuzzy modeling for a special map that exploits innovation usage of task navigation for real paths. Actually, visibility graphs based on the knowledge of human experts are employed to build FPE maps for navigation. To emphasize the idea of the created FPE, seven remarks direct the roadmap towards being a utility tool for robot navigation. Three illustrative examples, containing three spatial patterns, doors, corridors and cul-de-sacs, are also included. This paper paves the way to create ideas of intelligent navigation for further developments.

Keywords: Fuzzy modeling; Fuzzy set theory; Path planning; Robot navigation

1. Introduction

A fully autonomous robot needs a flexible map to solve frequent change of robot situations and/or tasks. Qualitative knowledge and topological information [16,17] are superior to the raw metric information [11] for building a spatial model that is compact and reproducible for task navigation. Qualitative spatial models in terms of a graph or topological map were developed and constructed to achieve the robustness and reproducibility of environment representation [3]. However, quantitative information providing precision navigation has its importance as well. A global topological map connecting local metric maps was proposed to allow a compact environment model, which does not require global metric consistency and permits both precision and robustness [40]. This paper focuses on developing a special map based on qualitative information flexibly combined with metric information to plan real paths for task navigation so that robots cope with the change of situation and/or tasks easily.

Robot navigation usually uses metric information for path planning. At the development initiation, Lozano-Pérez and Wesley [24] proposed a visibility graph to record both sets of all obstacle vertices and all connections for the two vertices without overlapping the obstacles in a workspace. For moving objects of polygon and polyhedron, Lozano-Pérez [23] presented algorithms to compute the configuration of the obstacle spaces and acquire a visibility graph. Because a visibility graph involves the information of collision-free paths, path planning becomes searching visibility graphs for the shortest path. Many researchers [1,26,30,44] then focused on developing more effective algorithms to search visibility graphs for the shortest path.

However, a visibility graph must be reconstructed when the sizes of moving objects vary. This reconstruction was eliminated by considering the maximum radius of collision-free regions in proposing voronoi diagrams [19]. In a voronoi diagram, the collision-free paths are equidistant from two or

☆ This research was supported by the National Science Council, Taiwan, ROC under Grants NSC-89-2213-E-146-003 and NSC-89-2218-E-146-003.
* Corresponding author. Tel.: +886 7 6011000x2810; fax: +886 7 6011239.
E-mail address: tuky@ccms.nkfust.edu.tw (K.-Y. Tu).

0921-8890/$ - see front matter © 2006 Elsevier B.V. All rights reserved.
doi:10.1016/j.robot.2006.04.001

more obstacle boundaries including the workspace boundary. Based on a voronoi diagram, a "retraction" method planned the path of a moving disc [27,28]. Moreover, Takahashi and Schilling proposed voronoi graphs for a moving rectangle [37]. Recorded in the voronoi graph, the collision-free paths stay away from the obstacles, but do not include the shortest path. Therefore, Liu and Arimoto applied the tangent graph idea [8,21,22] to an extended tangent graph [20] for finding the shortest path as a moving disc with arbitrary radius.

Both the visibility graph and the extended tangent graph solve the problem of visiting positions, namely path planning. However, controlling robots to pass the planned positions is the other problem, namely motion control. Path planning with a visibility graph or a tangent graph exhaustively searches its content to find the shortest or the safest path. Hence, both are called the global strategy of path planning problems. Global strategies are not adequate for real-time motion control because of usually wasting a very long time. In order to integrate motion control with path planning, Khatib [14] proposed the potential field approach to reduce the design procedure for real-time robot control.

The potential field approach usually designates obstacle positions as repulsive potential and a goal position as the minimum location of an attractive potential well in unobstructed environment [42]. On one hand, repulsive potential pushes a robot to stay away from an obstacle. On the other hand, an attractive potential well pulls a robot towards the minimum potential position, the goal position. Both repulsive and attractive potentials are combined to facilitate obstacle avoidance for real-time control.

In contrast to the global strategy, the potential field approach is called a local strategy because of only adopting a local view to model the environment around a robot. The form of mathematical equations makes it difficult in the potential field approach to add other information or to extend the active scope of robots. In addition, after planning, the global strategy fixes the traveled path, making it inflexible to a little change in environment. The strategies of both local and global path planning have their different shortcomings. By the navigation template, mediating qualitative guidance and quantitative control is a solution to the path planning possessing both precision and flexibility [32]. However, the combination of substrate and modifier navigation templates to calculate Preferred Direction of Travel (PDT) after the Immediate Navigation Objective (INO) is a difficult and complicated process for task navigation [32]. This paper proposes Fuzzy Potential Energy (FPE) which inherits the sprit of the potential field approach to gain the function that codes qualitative information into a quantitative value for robot navigation. The proposed FPE provides a simple way to plan real paths to finish a task.

FPE is an innovative application of fuzzy modeling to define a new type of potential field approach. Basically, there are two types of fuzzy modeling: (1) imitating an expert experiment or fulfilling engineering knowledge and (2) modeling a complex or unknown system. The function of the first type is similar to a controller [12,18,25,31,33,45,46]. The second type of fuzzy modeling is designed to approximate a complex or unknown system [5,6,10,15,29,34–36,38,39,43]. This type of fuzzy modeling is employed for controller design and/or for system analysis. When both engineering knowledge and an expert operation are insufficient, control laws can still be found. The FPE makes use of the second type of fuzzy modeling to construct spatial models for improving path-planning strategies. Khatib proposed a potential field approach to combine local strategy with the global strategy [14]. This combination considered only obstacle positions, which is usually used for global strategies, in local strategy. However, the obstacle positions are not unique information used for global strategies. There is lots of more important information such as obstacle vertices, connecting links between two vertices, junction nodes, terminal nodes and pseudo-nodes, etc., for different objectives of path planning. For example, the obstacle vertices and connecting links between two vertices are devised for the shortest path in a visibility graph [24]. Junction nodes, terminal nodes and pseudo-nodes are connected for the safest path in a voronoi diagram [37]. The proposed FPE facilitates the more important information to become useful in robot navigation.

Both local and global path planning navigate a robot for conducting a fixed task from its current position to a goal position. However, a fully autonomous robot, in general, selects one of many candidate tasks for conducting. Therefore, navigation after selecting one task needs quick algorithms to find the path in the given environment information for conducting. The FPE is defined to extend navigation functions from paths to tasks so that it can quickly find out the path for conducting a task. Compared with potential field approach, the FPE can locally adjust the potential distribution to improve the shortage of using the form of mathematical equations. Besides, the function of finding the path from qualitative information provides a way to quickly conduct task navigation. In addition, the workspace for FPE is divided into discrete cells like cell decomposition approaches [4,7,13,41]. Path planning approaches based on square cells can have the merits of generating accurate shortest paths, but they are inefficient when environments involve large areas of obstacle-free regions [4,41]. Quadtree-based approaches [7,13], in general, are more efficient than square grid-based approaches. The FPE makes use of the workspace based on the square grid-based approaches but having the function like quadtree-based approaches guiding forward neighborhood cells. The FPE approach makes a cell possess more sophisticate function that facilitates both easy reduction of the total number of cells in a workspace and flexible adjustment to solve robots for different tasks. The proposed FPE guides a robot using multiple directions like [2,9], but it trains by fuzzy rules and neural networks to obtain a robot's real paths, that are different from a visibility graph used to organize the distribution of FPEs in a workspace. According to visibility graphs, the FPE solving the problem of task navigation for real paths is much straighter. Three examples including three spatial patterns, a door, a corridor and a cul-de-sac, illustrate how to design the FPE for a special map that embeds a path to conduct its task. The main contribution of

this paper is to build a special map that is flexibly adjusted and easily maintained by FPEs.

The rest of this paper is organized as follows. In Section 2, FPE is defined to represent the potential energy of one position in a workspace. After assigning a variety of FPEs into distinct cells in a workspace, a map is built to form a potential function for robot navigation. It is derived that the gradient directions of a potential function can be used for navigating the robot in Section 3. For rigorously explaining the derived result, Section 3 is separated into two subsections to discuss the gradient directions of one FPE and the interaction between two FPEs, respectively. In Section 4, an FPE set in a workspace is proposed to ensure that the FPE can navigate a robot to arrive at a goal point. In Section 5, an FPE designed for paths to conduct tasks is presented by three examples. Besides how the FPE produces the path that avoids obstacles, and arrives at a goal position is also included. Conclusions and further development are discussed in Section 6.

2. Fuzzy potential energy for a spatial model

In this section, the FPE motivated by the potential field approach is defined. Based on this definition, FPE applications are formularized as three rules to construct spatial models for robot navigation. In addition, a computation scheme to get potential energy is also included.

Assume that FPE is defined for a two-dimensional workspace W, where W is divided into $(2q+1)^2$ square areas. The ijth square area is called cell $C_{i,j}$, where (i, j) is its central point, for i and $j = -q, \ldots, 0, \ldots, q$. Note that, in W, $C_{0,0}$ is the central cell, $C_{-q,q}$ is the top-left cell, $C_{q,q}$ is the top-right cell, $C_{-q,-q}$ is the bottom-left cell, and $C_{q,-q}$ is the bottom-right cell. An FPE is assigned to cells $C_{i,j}$ to contribute potential energy for robot navigation. The following expresses the assumptions about every cell.

Assumption A1. In the workspace W, every cell $C_{i,j}$, for i and $j = -q, \ldots, 0, \ldots, q$, is of unit length and width.

It is convenient for Assumption A1 to represent a workspace by FPEs, but this assumption will be relaxed for general workspaces at the ending of this section. That is, every cell can be not square, then W can be any size.

FPE is motivated by the potential field approach which, for robot navigation, constructs virtual potential energy at any position in W. The function of the virtual potential energy is to guide or affect a mobile robot so that it can avoid obstacles and go towards the goal position. To accomplish this objective, an obstacle associated with positive virtual potential energy results in repulsive force to push a mobile robot staying far away. In contrast, a goal point associated with negative energy results in attractive force to pull a mobile robot going towards its location. This idea leads us to define FPE.

FPE is defined using fuzzy set theory (FST) to produce the virtual potential energy. FST applications in general replace real variables with linguistic variables. A linguistic variable includes a term set, which is a set of names with linguistic values. Each linguistic value is quantified with a fuzzy set. For example, if ***speed*** is interpreted as a linguistic variable, then its term set ***T(speed)*** could be

$$\boldsymbol{T}(\boldsymbol{speed}) = \{slow, moderate, fast, very\ sloe, \\ more\ or\ less\ fast, \ldots\}, \quad (1)$$

where each term, the linguistic value in ***T(speed)*** is characterized by a fuzzy set. We might interpret "*slow*" as "a ***speed*** below about 40 mph", "*moderate*" as "a ***speed*** close to 55 mph", and "*fast*" as "a ***speed*** above about 70 mph". These terms can be characterized as fuzzy sets, $\tilde{F}_{\text{slow}}$, $\tilde{F}_{\text{moderate}}$ and $\tilde{F}_{\text{fast}}$, respectively. In all, the main constituents of FPE are linguistic variables and fuzzy sets.

Potential energy is viewed as a linguistic variable in the proposed FPE. Let the linguistic variable be named Potential Index (***PI***) and its term set be

$$\boldsymbol{T}(\boldsymbol{PI}) = \{k \mid k = -r, -r+1, \ldots, -1, 0, 1, \ldots r-1, r\}, \quad (2)$$

where r is the number of positive or negative ***PI***. The most positive (largest) ***PI*** is r, but the most negative (smallest) ***PI*** is $-r$. Thus, the number of the term set is $2r+1$. Moreover, the linguistic values are characterized by fuzzy sets $\tilde{P}_k$, for $k = -r, \ldots, 0, \ldots, r$ $(r > 0)$. Therefore, the FPE consists of both linguistic variables k, namely ***PI*** and fuzzy sets $\tilde{P}_k$. The following is a rigorous FPE description.

Definition 1 (*Fuzzy Potential Energy (FPE)*). FPE indicates potential energy with fuzzy sets. If ***PI*** of one region $\omega \in W$ is k, then the potential energy, dominated by this ***PI***, is represented by fuzzy set $\tilde{P}_k$, denoted by

$$\tilde{P}_k = \int_W \mu_{\tilde{P}_k}(x, y, R)/(x, y) \quad (3)$$

where W is the workspace, $(x, y) \in W$ is one position in the workspace, $\mu_{\tilde{P}_k}(x, y, R)$, the membership function of $\tilde{P}_k$, expresses the possibility of position (x, y) with ***PI*** k, and R is the parameter in the space limits covered by this membership function.

Note that $\tilde{P}_r$ is the largest FPE whereas $\tilde{P}_{-r}$ is the smallest FPE. In addition, $\{\tilde{P}_k, \text{for } k = -r+1, \ldots, -1\}$ are named moderate-negative FPEs, but $\{\tilde{P}_k, \text{for } k = r-1, \ldots, 1\}$ are named moderate-positive FPEs.

In FST, fuzzy sets are quantified by membership functions. Without exception, FPE $\tilde{P}_k$ requires a membership function to represent the quantity which is the possibility of potential energy k at one position covered by it. The following is the definition of membership functions.

Definition 2. The membership function $\mu_{\tilde{P}_k}(x, y, R)$.

If the FPE $\tilde{P}_k$ is assigned to the cell $C_{i,j}$, then $\mu_{\tilde{P}_k}(x, y, R) = \max(0, \mu_{P_k}(x, y, R))$, and

$$\begin{aligned}
&\mu_{P_k}(x, y, R) \\
&= 1 - 2(y-j)/3R \text{ when } (y-j) \geqq 3(x-i) \\
&\quad \text{and } (y-j) \geqq -3(x-i), \\
&= 1 - ((x-i) + (y-j))/2R \text{ when } (y-j) \geqq (x-i)/3 \\
&\quad \text{and } (y-j) \leqq 3(x-i),
\end{aligned}$$

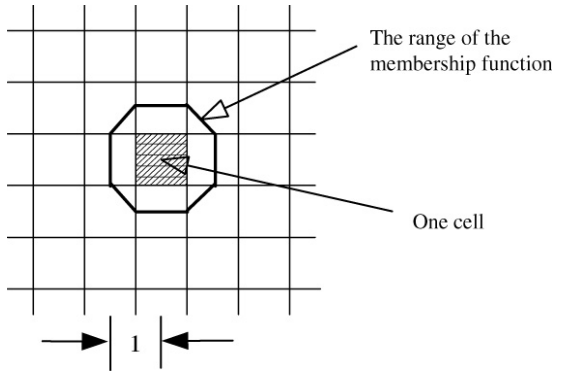

Fig. 1. The range of the membership function $\mu_{\tilde{P}_k}(x, y, 1)$.

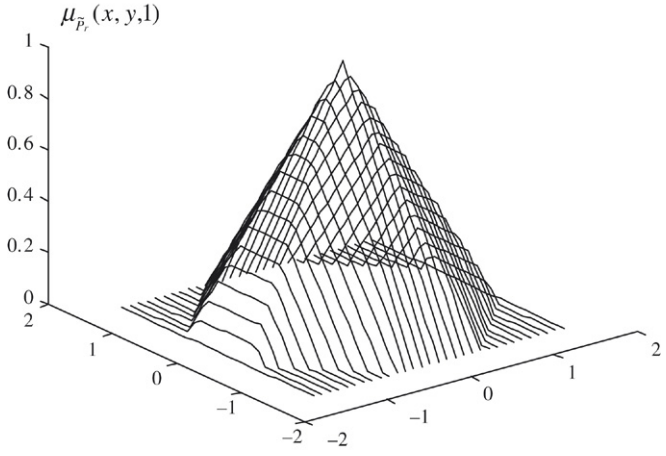

Fig. 2. The membership function $\mu_{\tilde{P}_r}(x, y, 1)$.

$$
\begin{aligned}
&= 1 - 2(x-i)/3R \text{ when } (y-j) \geqq -(x-i)/3 \\
&\quad \text{and } (y-j) \leqq (x-i)/3, \\
&= 1 - ((x-i) - (y-j))/2R \text{ when } (y-j) \geqq -3(x-i) \\
&\quad \text{and } (y-j) \leqq -(x-i)/3, \\
&= 1 + 2(y-j)/3R \text{ when } (y-j) \leqq 3(x-i) \\
&\quad \text{and } (y-j) \leqq -3(x-i), \\
&= 1 + ((x-i) + (y-j))/2R \text{ when } (y-j) \leqq (x-i)/3 \\
&\quad \text{and } (y-j) \geqq 3(x-i), \\
&= 1 + 2(x-i)/3R \text{ when } (y-j) \leqq -(x-i)/3 \\
&\quad \text{and } (y-j) \geqq (x-i)/3, \\
&= 1 + ((x-i) - (y-j))/2R \text{ when} \\
&\quad (y-j) \leqq -3(x-i) \text{ and } (y-j) \geqq -(x-i)/3, \qquad (4)
\end{aligned}
$$

where (i, j) is the central point of $C_{i,j}$, x and y are the vertical and horizontal positions, respectively. R is the distance between point (i, j) and one edge of the area covered by the FPE $\tilde{P}_k$.

Fig. 1 depicts the range of the membership function $\mu_{\tilde{P}_k}(x, y, 1)$. As shown in Fig. 1, $R = 1$, and the shaded square area is the cell occupied by FPE $\tilde{P}_k$. In addition, Fig. 2 shows the profile of $\mu_{\tilde{P}_k}(x, y, 1)$ as its center is at (0, 0). Fig. 2 reveals that the central position ($x = 0$ and $y = 0$) possesses the maximum membership grade. At the position leaving from its center, the membership grade degrades, and becomes zero as the position outside its cover range. Implied in Fig. 2, the central position has the maximum possibility of possessing ***PI*** k. The possibility degrades at the position leaving from its center, and the possibility becomes zero as the position becomes outside its range. The proposed FPE provides a way to represent the virtual potential energy (***PI***) under the continuity value (membership grade). This way lets FPE express virtual potential energy more flexibly than the potential field approach.

In respect of FPE functionality, the grade of $\mu_{\tilde{P}_k}(x, y, R)$ is the degree to which $\tilde{P}_k$ acts on a mobile robot at one position in the workspace. Thus, R means the FPE action range. Basically, FPE is proposed to have two types of action ranges because robot navigation faces two objects: obstacles and a goal position. During meeting an obstacle, a robot only needs to move far away from it. Therefore, the action range of one FPE designed for an obstacle only needs to involve its neighborhood cells. As shown in Fig. 1, $R = 1$ is this type of FPE. In contrast, a goal position needs effective action as a robot at any position in a workspace. Thus, R is proposed to be one half of the workspace length for a goal position. As a result, two types of membership functions, $\mu_{\tilde{P}_k}(x, y, 1)$ and $\mu_{\tilde{P}_k}(x, y, a)$ (where a is one half of the workspace length), are designated for the proposed FPE.

However, it is a design issue which cell in the workspace should possess which FPE. The design issue can be derived by the application rules of the potential field approach since FPE borrows its spirit. In general, the potential field approach is designed using rules in which the obstacle possesses the highest potential energy to push robots away from it, while the goal point possesses the lowest potential energy in order to pull robots towards it. In summary, the application rules for FPE are formularized as follows

Rule (1) If a cell $C_{i,j}$ covers the goal position, then its FPE is $\tilde{P}_{-r}$.
Rule (2) If a cell $C_{i,j}$ contains an obstacle, then its FPE is $\tilde{P}_r$.
Rule (3) If a cell $C_{i,j}$ needs a special effect on the mobile robot, then its FPE is $\tilde{P}_k$ (for $k = -r+1, \ldots, 0, \ldots, r-1$).

Rules (1) and (2) construct a basic navigation function of FPE that $\tilde{P}_{-r}$ guides towards a goal point, and $\tilde{P}_r$ for staying away from an obstacle. Rule (3) allows a planner to plan where a mobile robot goes through towards a goal point. From the point of view of energy, Rule (3) adds various levels of potential like injecting subjective actions on a mobile robot. The FPEs resulting in the subjective actions include two classifications: the moderate-negative FPEs ($\tilde{P}_k$, for $k = -r+1, \ldots, -1$) and the moderate-positive FPEs ($\tilde{P}_k$, for $k = 1, \ldots, r-1$). The moderate-negative FPEs result in attractive forces at various levels. In contrast, the moderate-positive FPEs result in repulsive forces at various levels. It is the advantage of the defined FPE that planners can use Rule (3) to flexibly adjust the potential energy distribution in a workspace. In this paper, the FPE assigned to the cells of a workspace builds a special map that can be flexibly adjusted by the moderate-negative FPEs. The moderate-negative FPEs locally adjusts potential distribution based on qualitative information in a workspace for a special task such as crossing a door, passing that corridor or

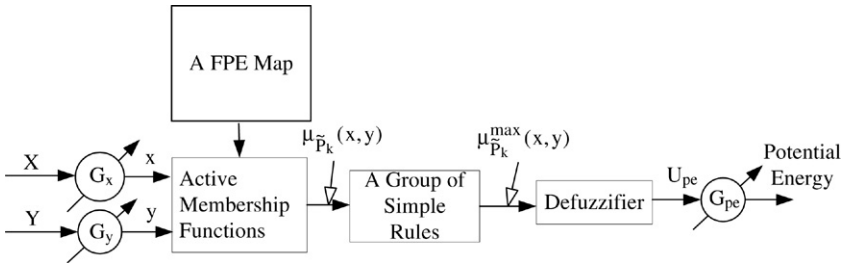

Fig. 3. A scheme of calculating potential energy.

escaping this cul-de-sac, etc. In Section 5, three spatial patterns will be contained in illustrative examples to demonstrate that the FPE can flexibly solve different navigation tasks.

Finally, guiding a robot needs a way to find the actual potential energy at any position in the entire workspace. Definition 1 reveals that when the cell $C_{i,j}$ possesses the FPE $\tilde{P}_k$, this cell's ***PI*** is k. This provides a sense to derive a group of simple rules as follows

$$\text{IF} \quad \text{the FPE is } \tilde{P}_k, \ \text{THEN} \quad \text{the potential energy is } k \tag{5}$$

where $\tilde{P}_k$ is the fuzzy set characterized by the membership function $\mu_{\tilde{P}_k}(\cdot)$, and k is ***PI*** (real value), for $k = -r \ldots, 0, \ldots, r$.

By the product operation rule of fuzzy implication and max aggregation operation, real potential energy at any position in the workspace can be obtained via a defuzzifier function, named the potential function hereafter, which is

$$U_{\text{pe}}(x, y) = \frac{\sum_{k=-r}^{r} \mu_{\tilde{P}_k}^{\max}(x, y)k}{\sum_{k=-r}^{r} \mu_{\tilde{P}_k}^{\max}(x, y)} \tag{6}$$

where $\mu_{\tilde{P}_k}^{\max}(x, y)$ is the maximum membership grade for all the fuzzy sets $\tilde{P}_k$, and $k = -r, \ldots, 0, \ldots, r$.

Note that a potential function constructed by FPE is a spatial map approach to a workspace for robot navigation.

Furthermore, a scheme for calculating the potential energy is formulated by Fig. 3, where (X, Y) is the position in the workspace, G_x and G_y are the normalizing scaling factors for X and Y, respectively, U_{pe} is the potential energy, and G_{pe} is the scaling factor for potential energy. Therefore,

$x = G_x X$,
$y = G_y Y$, and
Potential energy $= G_{\text{pe}} U_{\text{pe}}$.

In Fig. 3, the function of a group of simple rules associated with a defuzzifier is just to translate virtual energy into real potential energy. An FPE map plays the role of the calculation of kernel-like linguistic rules in a fuzzy logic controller. The FPE map dominates performance of a navigation work, and is usually built by the knowledge of human-expert-like linguistic rules in a fuzzy logic controller. In this paper, visibility graphs will be engaged as experts to build FPE maps. How a FPE map performs robot navigation will be revealed by analysis of FPE gradient directions in Section 3 to derive basic FPE layout in Section 4. In addition, there is still a little distinction from conventional fuzzy logic operation in the calculation scheme. Here variables x and y are inputs of all membership functions simultaneously, but input variables usually have distinct membership functions in conventional fuzzy logic operation. After taking the grade of all active membership functions, the simple rules and defuzzifier compute real potential energy U_{pe}. The calculation is a function of the form: $[-a, a]\times[-a, a] \to [-r, r]$, where a is half of the workspace's length or width, and r is the largest ***PI***. Note that G_x and G_y can be properly chosen such that the cells in the workspace are of unit length and width. For example, if the real size of a cell is 5×5 cm^2, then both G_x and G_y are $1/5$. In a workspace, the cells, which are of unit length and width, satisfy A1.

Remark 1. Each cell can be any size by appropriately choosing G_x and G_y.

3. The gradient directions of FPEs

How the FPE plays the role for robot navigation is analyzed by its gradient directions. This section derives the FPE gradient direction first, and then studies the gradient directions of both one FPE and interaction between two FPEs in two subsections, respectively.

It is well known that flow directions of an energy function are usually expressed by its gradient directions. Therefore, gradient directions of a potential function are regarded as acting directions of FPE on a mobile robot. Let the gradient directions be

$$\vec{\varepsilon}(x, y) = -\nabla U_{\text{pe}}(x, y) = -\frac{\partial U_{\text{pe}}}{\partial x}\hat{x} - \frac{\partial U_{\text{pe}}}{\partial y}\hat{y} \tag{7}$$

where $U_{\text{pe}}(x, y)$ is a potential function and $\hat{x}$ and $\hat{y}$ are the unit vectors in the x and y directions, respectively. Note that $\vec{\varepsilon}(x, y)$ is the potential field formed by the FPE in a workspace. In addition, see the equation in Box 1, where $\nabla\mu_{\tilde{P}_k}^{\max}(x, y)$ is the gradient of $\mu_{\tilde{P}_k}^{\max}(x, y)$, $\mu_{\tilde{P}_k}^{\max}(x, y)$ is the maximum grade of the membership function of all the fuzzy sets $\tilde{P}_k$, and k is ***PI***.

In general, the gradient direction of a real-value function at one point is the direction with the greatest increment. Here, the direction of minus gradient is that of the greatest decrement. That is, the gradient directions will avoid the high potential energy (the most positive FPE, possessed by an obstacle cell usually) and go towards the low potential energy (the most negative FPE, possessed by the goal point cell). Consequently, the definition of the gradient directions is consistent with the robot navigation objective.

$$\vec{\varepsilon}(x, y) = -\nabla \left(\frac{\sum_{k=-r}^{r} \mu_{\tilde{P}_k}^{\max}(x, y)k}{\sum_{k=-r}^{r} \mu_{\tilde{P}_k}^{\max}(x, y)} \right)$$
$$= \frac{\left(\sum_{k=-r}^{r} \mu_{\tilde{P}_k}^{\max}(\cdot)k \right) \left(\sum_{k=-r}^{r} \nabla\mu_{\tilde{P}_k}^{\max}(\cdot) \right) - \left(\sum_{k=-r}^{r} \nabla\mu_{\tilde{P}_k}^{\max}(\cdot)k \right) \left(\sum_{k=-r}^{r} \mu_{\tilde{P}_k}^{\max}(\cdot) \right)}{\left(\sum_{k=-r}^{r} \mu_{\tilde{P}_k}^{\max}(\cdot) \right)^2}$$

Box 1.

Because the membership functions of the negative FPEs cover the entire workspace, its FPE affects a mobile robot at any position inside the workspace. In contrast, the positive FPEs only affect a mobile robot within its neighborhood cells. In a word, the negative FPEs have wider applications than the positive FPE. Therefore, the study of gradient directions focuses on the negative FPEs. The positive FPE will be derived from these study results. The gradient of a potential function, as shown in the equation in Box 1, consists of that of the FPE membership functions. Thus, the gradient of one FPE membership function is regarded as its gradient. The gradient of both one negative FPE and the combination between two FPEs are studied in the next two subsections, respectively, for revealing FPE action in detail.

3.1. One negative FPE

In this subsection, the FPE discussed is the most negative FPE $\tilde{P}_{-r}$. The most negative FPE is able to create the minimum potential energy at one position where there is always the goal position of a moving robot, and is important for robot navigation. Therefore, $\tilde{P}_{-r}$ is discussed to reveal how to guide a robot towards a goal position.

There are eight sub-regions covered by the membership function $\mu_{\tilde{P}_{-r}}(\cdot)$ as shown in Fig. 2. In Fig. 2, the gradient directions are difference in each sub-region. Eight sub-regions are defined as follows for conveniently interpreting its gradient directions.

Definition 3. Let the FPE at cell $C_{i,j}$ be $\tilde{P}_{-r}$. Due to the membership function $\mu_{\tilde{P}_{-r}}(\cdot)$, W is divided into eight sub-regions W_m (for $m = 1, \ldots, 8$) as plotted in Fig. 4, where

W_1: when $(y - j) \geqq 3(x - i)$ and $(y - j) \geqq -3(x - i)$,
W_2: when $(y - j) \geqq (x - i)/3$ and $(y - j) \leqq 3(x - i)$,
W_3: when $(y - j) \geqq -(x - i)/3$ and $(y - j) \leqq (x - i)/3$,
W_4: when $(y - j) \geqq -3(x - i)$ and $(y - j) \leqq -(x - i)/3$,
W_5: when $(y - j) \leqq 3(x - i)$ and $(y - j) \leqq -3(x - i)$,
W_6: when $(y - j) \leqq (x - i)/3$ and $(y - j) \geqq 3(x - i)$,
W_7: when $(y - j) \leqq -(x - i)/3$ and $(y - j) \geqq (x - i)/3$,
W_8: when $(y - j) \leqq -3(x - i)$ and $(y - j) \geqq -(x - i)/3$.

The gradient directions of $\tilde{P}_{-r}$ are those of $\mu_{\tilde{P}_{-r}}(\cdot)$ as follows.

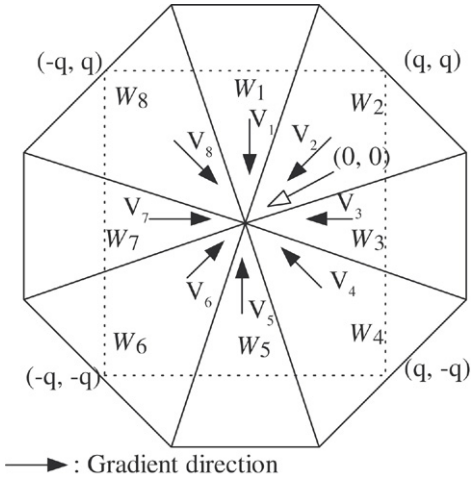

Fig. 4. The gradient directions of negative FPE $\tilde{P}_{-r}$.

Definition 4. The gradient directions of the negative FPE $\tilde{P}_{-r}$ are the gradient of its membership function $\mu_{\tilde{P}_{-r}}(\cdot)$. Let V_m be the gradient direction in W_m ($m = 1, \ldots, 8$). Then using Eq. (7) to calculate Eq. (4), the gradient directions of $\mu_{\tilde{P}_{-r}}(\cdot)$ are

$$V_1 = -(2/3a)\hat{y}, \quad V_2 = -(1/2a)\hat{x} - (1/2a)\hat{y},$$
$$V_3 = -(2/3a)\hat{x}, \quad V_4 = -(1/2a)\hat{x} + (1/2a)\hat{y},$$
$$V_5 = (2/3a)\hat{y}, \quad V_6 = (1/2a)\hat{x} + (1/2a)\hat{y},$$
$$V_7 = (2/3a)\hat{x}, \quad V_8 = (1/2a)\hat{x} - (1/2a)\hat{y},$$

where $\hat{x}$ and $\hat{y}$ are the unit vectors in the x and y directions, respectively, and a is one half of the workspace length.

As depicted in Fig. 4, the gradient directions of $\tilde{P}_{-r}$ point toward its central point which is always designated by the goal position. $\tilde{P}_{-r}$ thus results in an attractive force to pull the mobile robot toward its center. In contrast, FPE $\tilde{P}_r$, whose gradient directions point outward from its central point results in a repulsive force. Consequently, $\tilde{P}_{-r}$ can pull a mobile robot toward the goal position while $\tilde{P}_r$ can push a mobile robot to stay away from an obstacle.

Remark 2. An FPE guides via eight directions V_m, for $m = 1, \ldots, 8$, direction like quadtree-based approaches that a cell is divided into four sub-cells to express that a region is free or occupied by an obstacle. However, it is more sophisticated

that FPEs $\tilde{P}_k$ (for $k = -r, \ldots, 0, \ldots, r$) are of potential energy level $2 \times r + 1$ than that quadtree-based approaches distinguish each cell only by free or obstacle regions.

From Eq. (7), it is seen that it is insufficient for only one FPE to pull or push a mobile robot. Because one FPE has only one membership function, the membership functions of both numerator and denominator eliminate each other as seen in Eq. (7). Thus, the potential function becomes a constant value. The gradient of a constant value is zero that cannot navigate any mobile robot. A useful potential function should be constructed by more than one FPE. The next subsection will study the gradient directions of interaction between two negative FPEs in order to construct the ground of many FPEs forming a particular map.

3.2. Interaction between two negative FPEs

The gradient directions of two negative FPEs' interaction are described in the following property.

Property 1. *The gradient directions of interaction between any two negative FPEs point to the more negative FPE.*

Proof. Without lost generality, consider $\tilde{P}_{-r}$ and $\tilde{P}_{-r+j}$ (for $j = 1, \ldots, r-1$). From the equation in Box 1, $\tilde{P}_{-r}$ and $\tilde{P}_{-r+j}$ form a potential function as follows

$$\begin{aligned}
&\vec{\varepsilon}(x, y) \\
&= \frac{(\mu_{\tilde{P}_{-r+j}}(\cdot)(-r+j) + \mu_{\tilde{P}_{-r}}(\cdot)(-r))(\nabla\mu_{\tilde{P}_{-r+j}}(\cdot) + \nabla\mu_{\tilde{P}_{-r}}(\cdot))}{(\mu_{\tilde{P}_{-r+j}}(\cdot) + \mu_{\tilde{P}_{-r}}(\cdot))^2} \\
&\quad - \frac{(\mu_{\tilde{P}_{-r+j}}(\cdot) + \mu_{\tilde{P}_{-r}}(\cdot))(\nabla\mu_{\tilde{P}_{-r+j}}(\cdot)(-r+j) + \nabla\mu_{\tilde{P}_{-r}}(\cdot)(-r))}{(\mu_{\tilde{P}_{-r+j}}(\cdot) + \mu_{\tilde{P}_{-r}}(\cdot))^2} \\
&= \frac{-\mu_{\tilde{P}_{-r}}(\cdot)(j)\nabla\mu_{\tilde{P}_{-r+j}}(\cdot) + \mu_{\tilde{P}_{-r+j}}(\cdot)(r-1)\nabla\mu_{\tilde{P}_{-r}}(\cdot)}{(\mu_{\tilde{P}_{-r+j}}(\cdot)\mu_{\tilde{P}_{-r}})^2}. \qquad (8)
\end{aligned}$$

As shown in Eq. (8), the gradient of the potential function becomes that of $\mu_{\tilde{P}_{-r}}(\cdot)$ minus $\mu_{\tilde{P}_{-r+j}}(\cdot)$. That is, the gradient directions of $\tilde{P}_{-r}$ minus $\tilde{P}_{-r+j}$ are those of the interaction between $\tilde{P}_{-r}$ and $\tilde{P}_{-r+j}$.

Let FPEs $\tilde{P}_{-r}$ and $\tilde{P}_{-r+j}$ be assigned to $C_{0,0}$ and $C_{-q,q}$, respectively. Then, the cover range of $\mu_{\tilde{P}_{-r}}(\cdot)$ and $\mu_{\tilde{P}_{-r+j}}(\cdot)$ is respectively shown in Fig. 5. Fig. 5 also shows the overlapping region for $\mu_{\tilde{P}_{-r}}(\cdot)$ and $\mu_{\tilde{P}_{-r+j}}(\cdot)$. Inside the overlapping region, the membership grades of both FPEs have values simultaneously. Only inside this region both FPEs result in interaction. Thus, the gradient directions of interacting between $\tilde{P}_{-r}$ and $\tilde{P}_{-r+j}$ are studied by their overlapping regions only.

As shown in Fig. 5, the overlapping region is divided into fifteen sub-regions. Inside each one of the fifteen sub-regions, the gradient of $\mu_{\tilde{P}_{-r}}(\cdot)$ minus that of $\mu_{\tilde{P}_{-r+j}}(\cdot)$ are plotted in Fig. 6, respectively. In Fig. 6, the gradient directions point toward the central point of $\mu_{\tilde{P}_{-r}}(\cdot)$. That is, the central point of $\mu_{\tilde{P}_{-r}}(\cdot)$ is the aimed point of the interaction between FPEs $\tilde{P}_{-r}$ and $\tilde{P}_{-r+j}$. In summary, the gradient directions of the interaction between two negative FPEs ($\tilde{P}_{-r}$ and $\tilde{P}_{-r+j}$) point to the more negative FPE ($\tilde{P}_{-r}$). □

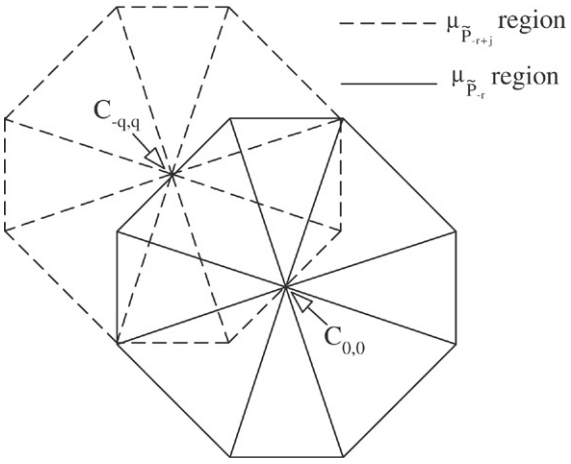

Fig. 5. The overlapping region of FPEs $\tilde{P}_{-r}$ and $\tilde{P}_{-r+j}$.

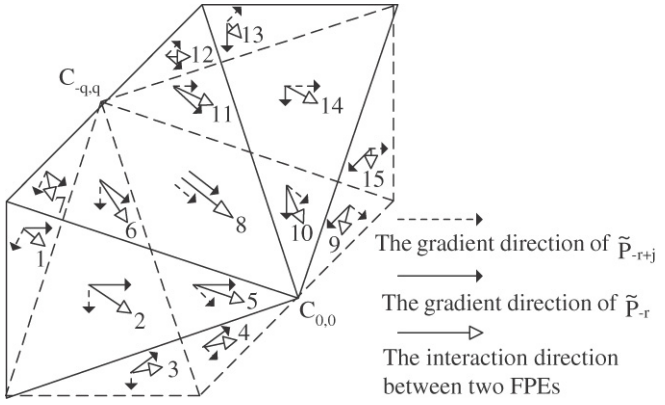

Fig. 6. The interaction directions between the FPEs $\tilde{P}_{-r}$ and $\tilde{P}_{-r+j}$.

Remark 3. Unlike the quadtree-based approach that a cell only has its individual action, either free or obstacle, any two cells based on the FPE approach can be designed to have interaction according to Property 1.

Property 1 is a main basis of assigning each FPE into a cell in order to propose an FPE set to ground a spatial model in the next section.

4. An FPE set

As mentioned above, only one FPE is unable to result in gradient lines for robot navigation. In this section, an FPE set stimulated for an applicable potential function is proposed and then is analyzed by its gradient directions to show it is adequate for robot navigation.

For robot navigation, the goal position designated with $\tilde{P}_{-r}$ is always devised to have the minimum potential energy. However, only one FPE does not result in an applicable potential function. For cooperating $\tilde{P}_{-r}$, the negative FPE $\tilde{P}_{-1}$ is thus designated at the position away from the goal position. This idea stimulates us to propose the FPE set as depicted in Fig. 7. Fig. 7 shows that $\tilde{P}_{-r}$ is assigned to the central cell $C_{0,0}$ which is the goal position, and four $\tilde{P}_{-1}$ are assigned to the four corner cells. From Property 1, the gradient directions of

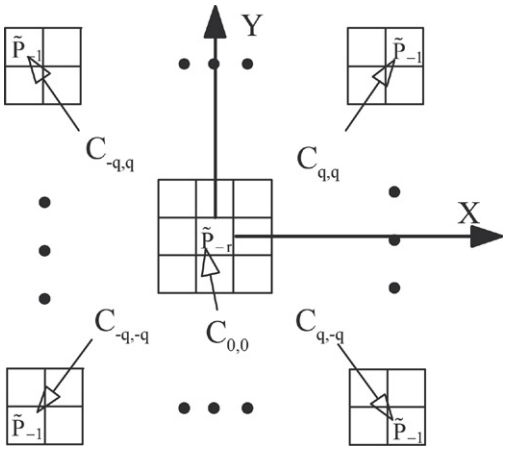

Fig. 7. An FPE set of the work space.

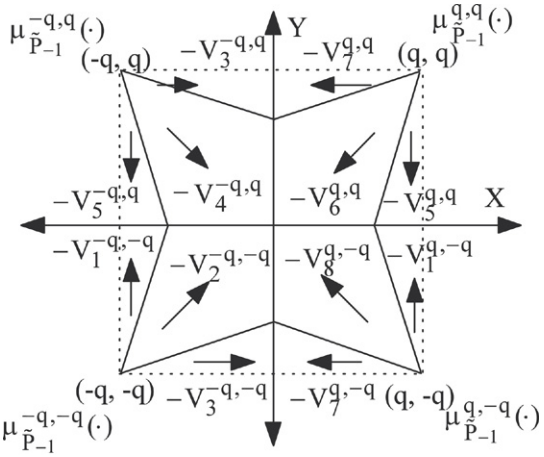

Fig. 8. Twelve sub-regions formed by four $\tilde{P}_{-1}$ in the workspace and the gradient direction in each sub-region.

the FPE set points toward the goal position which possesses the minimum FPE $\tilde{P}_{-r}$. The gradient lines how to go ahead towards the goal position from anywhere in the workspace are presented by rigorous analysis as follows.

In Fig. 7, there are four FPEs $\tilde{P}_{-1}$. Four $\tilde{P}_{-1}$ will be distinguished by their location under the following definition.

Definition 5. Let $\tilde{P}_{-1}$ located at $C_{i,j}$ be represented by $\tilde{P}_{-1}^{i,j}$. Then its membership function is expressed by $\mu_{\tilde{P}_{-1}}^{i,j}(\cdot)$. In addition, $W_m^{i,j}$ (for $m = 1, \ldots, 8$) are the eight sub-regions covered by the membership function, and $V_m^{i,j}$ is the gradient direction inside $W_m^{i,j}$ ($m = 1, \ldots, 8$).

Next, the gradient directions of the potential function formed by the FPE set are studied. Because of one FPE $\tilde{P}_{-r}$ and four FPEs $\tilde{P}_{-1}$ in W, the equation in Box 1 becomes

$$\begin{aligned}
&\vec{\varepsilon}(x, y) \\
&= \frac{(\mu_{\tilde{P}_{-1}}^{\max}(\cdot)(-1) + \mu_{\tilde{P}_{-r}}(\cdot)(-r))(\nabla\mu_{\tilde{P}_{-1}}^{\max}(\cdot) + \nabla\mu_{\tilde{P}_{-r}}(\cdot))}{(\mu_{\tilde{P}_{-r}}(\cdot) + \mu_{\tilde{P}_{-1}}^{\max}(\cdot))^2} \\
&\quad - \frac{(\mu_{\tilde{P}_{-1}}^{\max}(\cdot) + \mu_{\tilde{P}_{-r}}(\cdot))(\nabla\mu_{\tilde{P}_{-1}}^{\max}(\cdot)(-1) + \nabla\mu_{\tilde{P}_{-r}}(\cdot)(-r))}{(\mu_{\tilde{P}_{-r}}(\cdot) + \mu_{\tilde{P}_{-1}}^{\max}(\cdot))^2} \\
&= \frac{-\mu_{\tilde{P}_{-r}}(\cdot)(r-1)\nabla\mu_{\tilde{P}_{-1}}^{\max}(\cdot) + \mu_{\tilde{P}_{-1}}^{\max}(\cdot)(r-1)\nabla\mu_{\tilde{P}_{-r}}(\cdot)}{(\mu_{\tilde{P}_{-r}}(\cdot) + \mu_{\tilde{P}_{-1}}^{\max}(\cdot))^2}
\end{aligned} \tag{9}$$

where $\mu_{\tilde{P}_{-1}}^{\max}(x, y)$ is the maximum grade of the membership functions of all fuzzy sets $\tilde{P}_{-1}$, and $\nabla\mu_{\tilde{P}_{-1}}^{\max}(x, y)$ is the gradient of $\mu_{\tilde{P}_{-1}}^{\max}(x, y)$.

The gradient directions can be divided into two classes: the interaction between the FPEs $\tilde{P}_{-r}$ and $\tilde{P}_{-1}$ and the interaction between two FPEs $\tilde{P}_{-1}$ which are located at different positions. The first class was solved using Property 1, namely the interaction directions from $\tilde{P}_{-1}$ to $\tilde{P}_{-r}$. The second class can be investigated by the first term of the numerator in Eq. (9), $-\mu_{\tilde{P}_{-r}}(\cdot)(r-1)\nabla\mu_{\tilde{P}_{-1}}^{\max}(\cdot)$. Because there are four FPEs $\tilde{P}_{-1}$ in the workspace,

$$\nabla\mu_{\tilde{P}_{-1}}^{\max}(\cdot) = \nabla\left\{\max\left(\mu_{\tilde{P}_{-1}}^{q,q}, \mu_{\tilde{P}_{-1}}^{-q,q}, \mu_{\tilde{P}_{-1}}^{-q,-q}, \mu_{\tilde{P}_{-1}}^{q,-q}\right)\right\}, \tag{10}$$

where $\mu_{\tilde{P}_{-1}}^{i,j}(\cdot)$ is the membership function of the FPE $\tilde{P}_{-1}$ assigned to the cell $C_{i,j}$, for i and $j = -q$ or q. This term shows that the interaction directions between two FPEs $\tilde{P}_{-1}$ are $-\nabla\mu_{\tilde{P}_{-1}}^{\max}(\cdot)$. $-\nabla\mu_{\tilde{P}_{-1}}^{\max}(\cdot)$ is stated by the following property.

Property 2. *In the FPE set, the gradient directions of four FPEs $\tilde{P}_{-1}$ satisfy the following statements*

(i) *The membership functions $\mu_{\tilde{P}_{-1}}^{\max}(\cdot)$ divide the workspace into twelve sub-regions.*

(ii) *Let three sub-regions covered by the same membership function in one corner cell be a group (e.g. $-V_1^{-q,-q}$, $-V_2^{-q,-q}$ and $-V_3^{-q,-q}$ belong to the group $\tilde{P}_{-1}^{-q,-q}$). Then, the gradient directions $-\nabla\mu_{\tilde{P}_{-1}}^{\max}(\cdot)$ of the same group point outward the center of its corner cell as depicted in Fig. 8.*

Proof. Four membership functions $\mu_{\tilde{P}_{-1}}^{i,j}(\cdot)$ ($i, j = -q$ or q) intersect on the horizontal or vertical line. For example, $\mu_{\tilde{P}_{-1}}^{-q,-q}(\cdot)$ intersects with $\mu_{\tilde{P}_{-1}}^{q,-q}(\cdot)$ on the vertical line and with $\mu_{\tilde{P}_{-1}}^{-q,q}(\cdot)$ on the horizontal line, respectively. In the workspace, there are four areas thus dominated by $\mu_{\tilde{P}_{-1}}^{q,q}(\cdot)$, $\mu_{\tilde{P}_{-1}}^{-q,q}(\cdot)$, $\mu_{\tilde{P}_{-1}}^{-q,-q}(\cdot)$, and $\mu_{\tilde{P}_{-1}}^{q,-q}(\cdot)$, respectively. The top-right area is dominated by $\mu_{\tilde{P}_{-1}}^{q,q}(\cdot)$, the top-left area is dominated by $\mu_{\tilde{P}_{-1}}^{-q,q}(\cdot)$, the bottom-right area is dominated by $\mu_{\tilde{P}_{-1}}^{q,-q}(\cdot)$, and the bottom-left area is dominated by $\mu_{\tilde{P}_{-1}}^{-q,-q}(\cdot)$. Therefore, inside the bottom-left area, Eq. (10) becomes

$$\mu_{\tilde{P}_{-1}}^{\max}(\cdot) = \max\left(\mu_{\tilde{P}_{-1}}^{q,q}, \mu_{\tilde{P}_{-1}}^{-q,q}, \mu_{\tilde{P}_{-1}}^{-q,-q}, \mu_{\tilde{P}_{-1}}^{q,-q}\right) = \mu_{\tilde{P}_{-1}}^{-q,-q}.$$

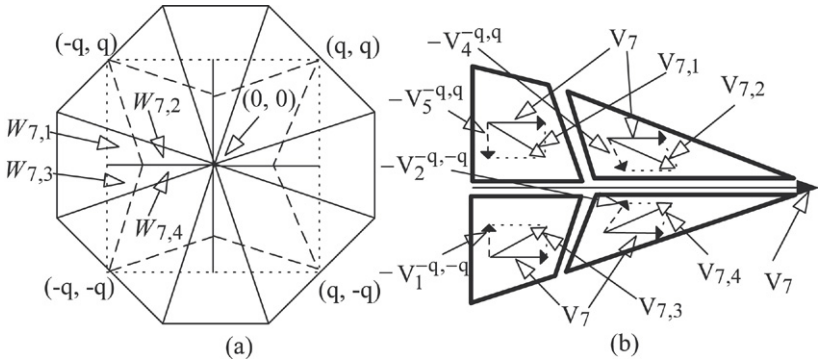

Fig. 9. The gradient directions of the FPE set in W_7.

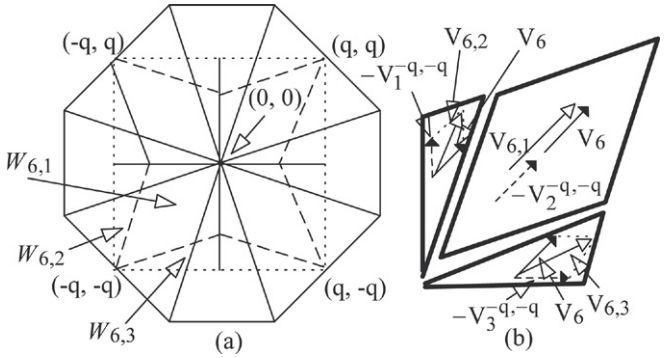

Fig. 10. The gradient directions of the FPE set inside W_6.

In addition, each area is separated by its membership function into three sub-regions. For example, in the bottom-left area, the range of $\mu_{\tilde{P}_{-1}}^{-q,-q}$ is separated into $W_1^{-q,-q}$, $W_2^{-q,-q}$ and $W_3^{-q,-q}$. The workspace is thus divided into twelve regions. Statement (i) is then proven.

In each sub-region, the gradient directions of the FPE $\tilde{P}_{-1}$ can be found from the gradient directions of dominating membership function. From Definition 5, the gradient directions $-\nabla\mu_{\tilde{P}_{-1}}^{\max}(\cdot)$ equal $-V_m^{i,j}$, for $i, j = -q$ or q, and $m = 1, \ldots, 8$. For instance, in the sub-regions $W_1^{-q,-q}$, $W_2^{-q,-q}$ and $W_3^{-q,-q}$, the gradient directions of the FPE $\tilde{P}_{-1}$, $-\nabla\mu_{\tilde{P}_{-1}}^{-q,-q}(\cdot)$ are $-V_1^{-q,-q}$, $-V_2^{-q,-q}$ and $-V_3^{-q,-q}$, respectively. Fig. 8 depicts the gradient directions in each sub-region. Statement (ii) is also proven. □

Finally, Properties 1 and 2 are utilized for analyzing the gradient directions of the FPE set by dividing the workspace into eight regions, W_m (for $m = 1, \ldots, 8$), as plotted in Fig. 4. Because the gradient directions of these eight regions have symmetrical relationship, the following property only analyzes regions W_6 and W_7. The rest of the regions can be derived from the following property.

Property 3. *Let W_6 and W_7 be divided into $W_{7,j}$ and $W_{6,i}$ ($j = 1, \ldots, 4$, and $i = 1, 2, 3$), as depicted in Figs. 9 and 10, respectively. The gradient directions of the FPE set in W_6 and W_7 point toward $(0, 0)$ in the following cases:*

Case (1): *Inside W_7 or $W_{6,2}$, the gradient directions point toward the horizontal line and then along the horizontal line toward* $(0, 0)$.

Case (2): *Inside $W_{6,3}$, the gradient directions point toward the vertical line and then along the vertical line toward* $(0, 0)$.

Case (3): *Inside $W_{6,1}$, the gradient directions point toward* $(0, 0)$ *directly.*

Proof. Case (1): This is about the gradient directions in W_7 and $W_{6,2}$, respectively. Firstly, inside the sub-region W_7, we have

$$\mu_{\tilde{P}_{-1}}^{-q,q}(\cdot) > \mu_{\tilde{P}_{-1}}^{q,-q}(\cdot), \quad \mu_{\tilde{P}_{-1}}^{-q,q}(\cdot) > \mu_{\tilde{P}_{-1}}^{q,q}(\cdot)$$
$$\mu_{\tilde{P}_{-1}}^{-q,-q}(\cdot) > \mu_{\tilde{P}_{-1}}^{q,-q}(\cdot), \quad \text{and} \quad \mu_{\tilde{P}_{-1}}^{-q,-q}(\cdot) > \mu_{\tilde{P}_{-1}}^{q,q}(\cdot)$$

where $\mu_{\tilde{P}_{-1}}^{i,j}(\cdot)$ is the membership function of the FPE $\tilde{P}_{-1}$ in $C_{i,j}$ $(i, j = -q, q)$. Therefore,

$$\mu_{\tilde{P}_{-1}}^{\max}(\cdot) = \max\left(\mu_{\tilde{P}_{-1}}^{q,q}, \mu_{\tilde{P}_{-1}}^{-q,q}, \mu_{\tilde{P}_{-1}}^{-q,-q}, \mu_{\tilde{P}_{-1}}^{q,-q}\right) = \max\left(\mu_{\tilde{P}_{-1}}^{-q,q}(\cdot), \mu_{\tilde{P}_{-1}}^{-q,-q}(\cdot)\right).$$

$W_{7,1}$ and $W_{7,2}$ belong to the top-left area of the workspace, and are dominated by $\mu_{\tilde{P}_{-1}}^{-q,q}$. Similarly, $W_{7,3}$ and $W_{7,4}$ are dominated by $\mu_{\tilde{P}_{-1}}^{-q,-q}$. Thus,

$$\mu_{\tilde{P}_{-1}}^{\max}(x, y) = \mu_{\tilde{P}_{-1}}^{-q,q}(x, y) \quad \text{if } (x, y) \in W_{7,1} \text{ or } W_{7,2},$$

and

$$\mu_{\tilde{P}_{-1}}^{\max}(x, y) = \mu_{\tilde{P}_{-1}}^{-q,-q}(x, y) \quad \text{if } (x, y) \in W_{7,3} \text{ or } W_{7,4}.$$

Moreover, $\nabla\mu_{\tilde{P}_{-r}} = V_7$. As depicted in Fig. 8,

$$-\nabla\mu_{\tilde{P}_{-1}}^{i,j}(x, y) = -V_m^{i,j} \quad \text{if } (x, y) \in W_m^{i,j} \quad (i, j = -q \text{ or } q \text{ and } m = 1, \ldots, 8). \tag{11}$$

Therefore, Eq. (9) becomes

$$\vec{\varepsilon}(x, y) = \frac{-\mu_{\tilde{P}_{-r}}(\cdot)(r-1)V_m^{i,j} + \mu_{\tilde{P}_{-1}}^{\max}(\cdot)(r-1)V_7}{\left(\sum_{k=-r,-1}\mu_{\tilde{P}_k}^{\max}(\cdot)\right)^2} \tag{12}$$

($m = 4, 5$ if $(i, j) = (-q, q)$; $m = 1, 2$ if $(i, j) = (-q, -q)$). As shown in Fig. 9(a), $W_{7,1}$ overlaps with $W_5^{-q,q}$. Thus, $V_m^{i,j} = V_5^{-q,q}$. Substituting the result into Eq. (12), we have

$$\vec{\varepsilon}(x, y) = \frac{-\mu_{\tilde{P}_{-r}}(\cdot)(r-1)V_5^{-q,q} + \mu_{\tilde{P}_{-1}}^{\max}(\cdot)(r-1)V_7}{\left(\sum_{k=-r,-1}\mu_{\tilde{P}_k}^{\max}(\cdot)\right)^2}. \quad (13)$$

Eq. (13) implies that inside $W_{7,1}$, the gradient directions are the sum of the vectors $-V_5^{-q,q}$ and V_7. This result is $V_{7,1}$ as shown in Fig. 9(b). Similarly, $V_{7,2}$, $V_{7,3}$, and $V_{7,4}$ are the gradient directions of the FPE set inside $W_{7,2}$, $W_{7,3}$, and $W_{7,4}$, respectively. In Fig. 9(b), $V_{7,i}$ $(i = 1, \ldots, 4)$ show that the gradient directions of the FPE set inside W_7 point at the horizontal line and then go along the horizontal line toward (0, 0).

Secondly, inside $W_{6,2}$, we have

$$\mu_{\tilde{P}_{-1}}^{-q,-q}(\cdot) > \mu_{\tilde{P}_{-1}}^{q,-q}(\cdot), \quad \mu_{\tilde{P}_{-1}}^{-q,-q}(\cdot) > \mu_{\tilde{P}_{-1}}^{q,q}(\cdot), \quad \text{and}$$
$$\mu_{\tilde{P}_{-1}}^{-q,-q}(\cdot) > \mu_{\tilde{P}_{-1}}^{-q,q}(\cdot).$$

Thus,

$$\mu_{\tilde{P}_{-1}}^{\max}(\cdot) = \mu_{\tilde{P}_{-1}}^{-q,-q}(\cdot), \quad \text{and}$$
$$-\nabla\mu_{\tilde{P}_{-1}}^{\max} = -\mu_{\tilde{P}_{-1}}^{-q,-q} = -V_1^{-q,-q}. \quad (14)$$

Because $W_{6,2}$ belongs to W_6,

$$\nabla\mu_{\tilde{P}_{-r}} = V_6. \quad (15)$$

Substituting (14) and (15) into (9), we have

$$\vec{\varepsilon}(x, y) = \frac{-\mu_{\tilde{P}_{-r}}(\cdot)(r-1)V_1^{-q,-q} + \mu_{\tilde{P}_{-1}}^{\max}(\cdot)(r-1)V_6}{\left(\sum_{k=-r,-1}\mu_{\tilde{P}_k}^{\max}(\cdot)\right)^2}. \quad (16)$$

Eq. (16) shows that inside $W_{6,2}$, the gradient direction $V_{6,2}$, as depicted in Fig. 10(b), is the summation of the vectors $-V_1^{-q,-q}(\cdot)$ and V_6, which goes toward $W_{7,3}$. As shown in Fig. 9(b), the gradient directions of the FPE set in $W_{7,3}$ point at the horizontal line and then follow the horizontal line toward the goal point. Thus, inside $W_{7,3}$, $W_{6,2}$, the gradient directions point at the horizontal line and then follow the horizontal line toward the goal point.

Case (2): This is about the gradient directions inside the subregion $W_{6,3}$, which belongs to $W_3^{-q,-q}$. Thus,

$$\mu_{\tilde{P}_{-1}}^{\max}(\cdot) = \mu_{\tilde{P}_{-1}}^{-q,-q}(\cdot), \quad \text{and}$$
$$-\nabla\mu_{\tilde{P}_{-1}}^{\max} = -\nabla\mu_{\tilde{P}_{-1}}^{-q,-q} = -V_3^{-q,-q}. \quad (17)$$

Substituting (17) into (9), we have

$$\vec{\varepsilon}(x, y) = \frac{-\mu_{\tilde{P}_{-r}}(\cdot)(r-1)V_3^{-q,-q} + \mu_{\tilde{P}_{-1}}^{\max}(\cdot)(r-1)V_6}{\left(\sum_{k=-r,-1}\mu_{\tilde{P}_k}^{\max}(\cdot)\right)^2}. \quad (18)$$

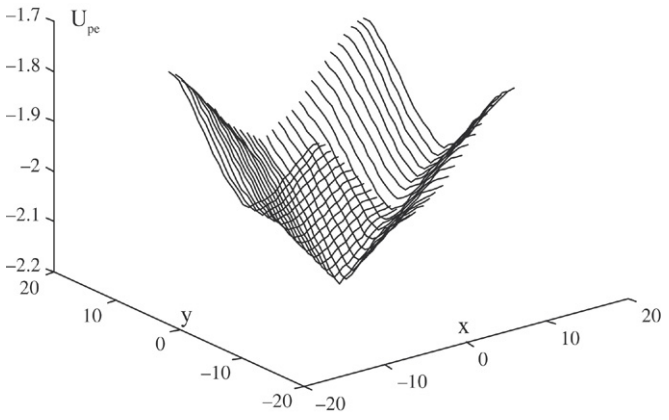

Fig. 11. The potential energy distribution of the FPE set in the workspace.

Eq. (18) shows that the gradient directions $V_{6,3}$ as depicted in Fig. 10(b) are the summation of $-V_3^{-q,-q}(\cdot)$ and V_6, which points at the vertical line and then follows the vertical line toward (0, 0).

Case (3): This is case about the gradient directions inside $W_{6,1}$. In this region, we have

$$\mu_{\tilde{P}_{-1}}^{\max}(\cdot) = \mu_{\tilde{P}_{-1}}^{-q,-q}(\cdot), \quad \text{and}$$
$$-\nabla\mu_{\tilde{P}_{-1}}^{\max} = -\nabla\mu_{\tilde{P}_{-1}}^{-q,-q} = -V_2^{-q,-q}. \quad (19)$$

In addition,

$$\nabla\mu_{\tilde{P}_{-r}} = V_6, \quad \text{and}$$
$$V_6 = -V_2^{-q,-q}. \quad (20)$$

(Both in same direction as shown in Fig. 10(b).)

Substituting Eqs. (19) and (20) into Eq. (9), we have

$$\vec{\varepsilon}(x, y) = \frac{-\mu_{\tilde{P}_{-r}}(\cdot)(r-1)V_2^{-q,-q} + \mu_{\tilde{P}_{-1}}^{\max}(\cdot)(r-1)V_6}{\left(\sum_{k=-r,-1}\mu_{\tilde{P}_k}^{\max}(\cdot)\right)^2}$$
$$= \frac{[\mu_{\tilde{P}_{-r}}(\cdot)(r-1) + \mu_{\tilde{P}_{-1}}^{\max}(\cdot)(r-1)]V_6}{\left(\sum_{k=-r,-1}\mu_{\tilde{P}_k}^{\max}(\cdot)\right)^2}. \quad (21)$$

Eq. (21) shows that inside $W_{6,1}$, the gradient direction V_6 directly points toward (0, 0) as depicted in Fig. 10(b). □

Property 3 can be extended to take the gradient directions of the FPE set inside the rest regions, $W_1, \ldots, W_5$, and W_8. The gradient directions inside W_3 are similar to those inside W_7, but pointing toward (0, 0) from different directions: one from right to left (inside W_3), and the other from left to right (inside W_7). W_1 and W_5 are also similar to W_7, but the gradient directions point toward the vertical line and then follow it toward (0, 0). In addition, W_2, W_4, and W_8 are similar to W_6. In the entire workspace, the gradient directions of the FPE set are thus obtained. From the computer simulations, Fig. 11 is the potential energy distribution of the FPE set in the workspace,

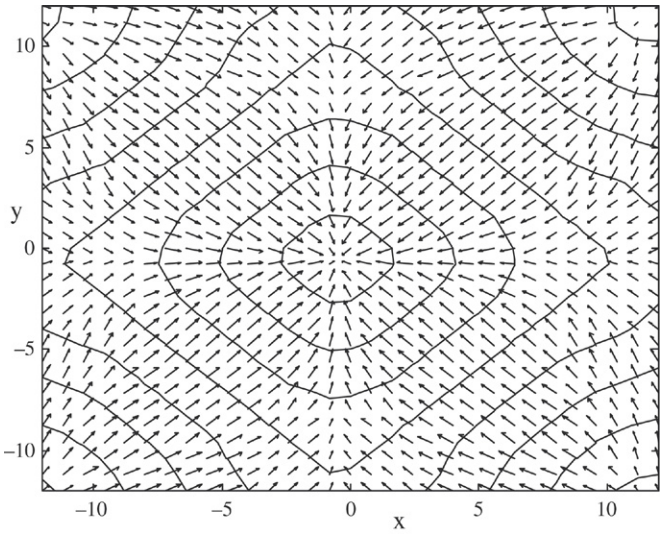

Fig. 12. The gradient directions of the FPE set in the workspace.

and Fig. 12 is the gradient directions of the FPE set. Simulation results also demonstrate the FPE set can navigate a mobile robot toward (0, 0), the goal position.

The FPE set grounds a special map using FPEs $\tilde{P}_{-1}$ and $\tilde{P}_{-r}$. There are four $\tilde{P}_{-1}$ and one $\tilde{P}_{-r}$ in the map that can guide a mobile robot towards the goal point $C_{0,0}$ from any direction. In a practice application, a map built does not need four $\tilde{P}_{-1}$s, but only one $\tilde{P}_{-1}$ and one $\tilde{P}_{-r}$ are enough to form a guide field. The application examples in the next section just use one $\tilde{P}_{-1}$ and one $\tilde{P}_{-r}$ to ground the basis of a map. Other FPEs are designated at the other cells in the map to guide a mobile robot for avoiding obstacles and then going towards a goal point.

The map contains cells $(2 \times q + 1)^2$ to store environment information. Such an approach like [13] uses square grid cells, but the cells containing an FPE result in more sophisticated functions to guide robots. The functions include two kinds. The first kind is one FPE action that guides robots to approach a negative one and/or to leave a positive one via eight directions V_j, for $j = 1, \ldots, 8$. A function of this kind is similar to a quadtree-based approach that guides forward only four near cells like four directions. It is more efficient to guide robots in eight directions by the FPE approach. The second kind is the interaction between two different FPEs that guides from large to small as seen in Property 1. A function of this kind is similar to a framed-quadtree approach [7] that guides from one cell to other cells. Compared to a framed-quadtree approach that guides towards other cells via the cell boundary, it is more flexible that the FPE guides via vector summation of two FPE gradient directions.

Remark 4. The FPE approach to robot navigation builds a map that FPEs are assigned to the cells between $\tilde{P}_{-1}$ and $\tilde{P}_{-r}$ to form a potential energy distribution map by which a mobile robot can be guided to leave obstacles and then to go towards a goal position. It is convenient to plan tasks by assigning FPEs into the cell in a workspace for the navigation path. The next section will explain how to extend the planning of the path to that of tasks.

5. FPE design for the planning of path and tasks

In this section, FPEs are classified for conveniently constructing FPE maps. The detailed design is shown step by step by constructing maps to present how to solve different tasks in the same environment situations. Gradient trajectories (the planned paths) showing how to guide a mobile robot towards the goal point are also included.

FPE can be separated into three classes. The first class is the negative FPEs $\tilde{P}_{-r}$ and $\tilde{P}_{-1}$ that are used for the proposed FPE set as described in the previous section. As shown in Property 3, the FPE set results in a potential function whose gradient directions point towards the goal point. The second class is the positive FPE $\tilde{P}_r$ that is applied to push a mobile robot so that it stay away from obstacles. The third class is the moderate-negative FPEs $\tilde{P}_k$ (for $k = -r + 1, \ldots, -2$) that are employed to adjust the potential energy distribution between $\tilde{P}_{-r}$ and $\tilde{P}_{-1}$. Relying on Property 1, the moderate-negative FPEs of distinct level are located at the different cells where a mobile robot would like to finish a sequence move for a task. For showing the merits of design of the moderate-negative FPEs, there are three examples in the following: the first example for navigating to cross a door or a corridor; the second example for navigation to avoid or to escape a cul-de-sac; and the last example for navigation to conduct a sequence of tasks. The third class of FPE design shows the main contribution of this paper.

Example 1. Navigation for crossing a door or a corridor.

This example demonstrates that it is easy to conduct the tasks for crossing a door or a corridor by Figs. 13 and 14, respectively. As shown in Fig. 13(a), the cells occupied by the corridor or the door are assigned by $\tilde{P}_r$ to push mobile robots far away. For guiding mobile robots going through the corridor, the goal position cell $C_{-3,-2}$ and its entrance cell $C_{-3,-8}$ are assigned by $\tilde{P}_{-r}$ and $\tilde{P}_{-2}$, respectively, to form gradient lines that do not cross the door. Fig. 13(b) shows the gradient trajectories as the desired planning exactly cross the corridor without hitting obstacles, the corridor and the door. Moreover, for guiding a mobile robot going the other way, through the door, the goal cell $C_{-8,-2}$ and the door entrance cell $C_{-8,-8}$ are assigned by $\tilde{P}_{-r}$ and $\tilde{P}_{-2}$, respectively, as shown in Fig. 14(a). The gradient trajectories, as shown in Fig. 14(b), cross through the door as the desired planning.

Remark 5. The qualitative information such as a door, a corridor and their entrances can be lent to navigate a mobile robot for conducting the tasks, crossing either a door or a corridor. Besides, task navigation exactly results in appropriate paths. A map built by the FPE provides a way to make use of qualitative information for appropriate paths guiding a mobile robot to arrive at a goal position.

Example 2. Navigation for avoiding or escaping a cul-de-sac.

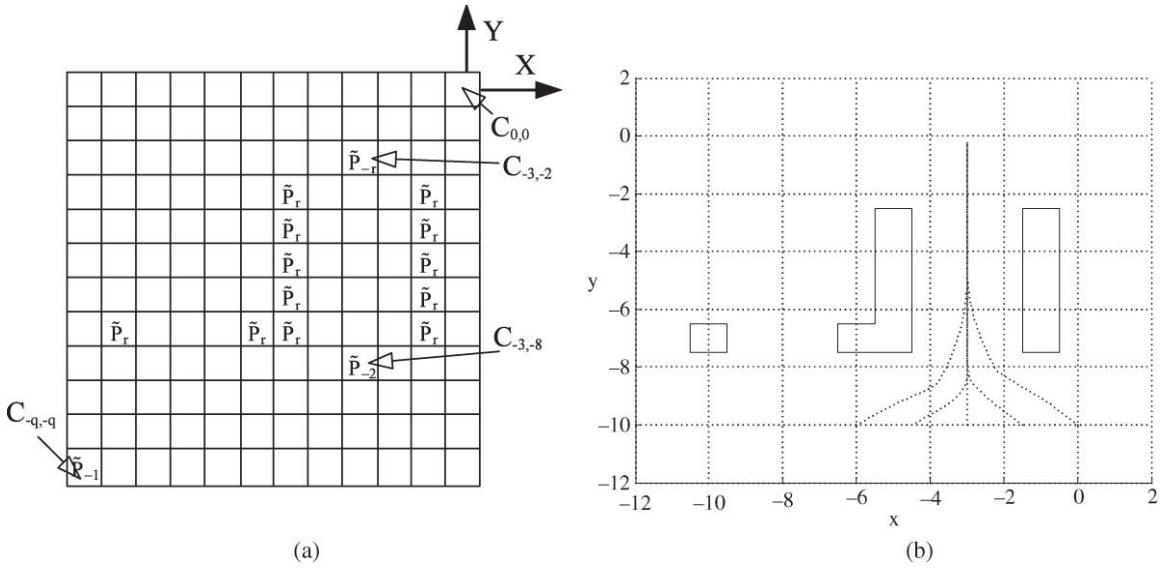

Fig. 13. FPE layout and gradient lines for going through a corridor.

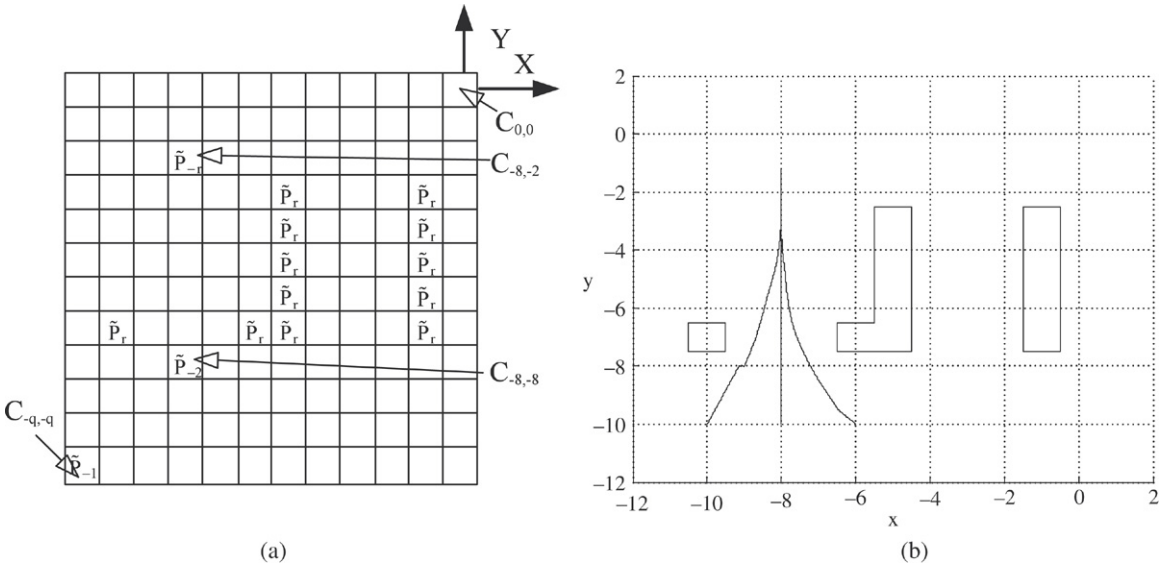

Fig. 14. FPE layout and gradient lines for going through a door.

There are two situations discussed in the example: the mobile robot inside or outside the cul-de-sac. As outside, the task of navigation is to guide a mobile robot going around the cul-de-sac for a goal position. But, that of navigation from inside is a guide for escaping the cul-de-sac and then for going to a goal position. This example illustrates that it is very simple for the FPE to solve these two distinct tasks under different situations.

As outside, preventing a mobile robot from entering the cul-de-sac obstacle and then guiding towards the goal position are the task of navigation. However, many paths satisfy this requirement. Selecting the paths becomes the key-point of the moderate-negative FPEs' design. Here a visibility graph, the shortest path of global path planning strategy, is cited to select such a path as shown in Fig. 15. In Fig. 15, the dashed lines are the shortest path for avoiding the U-shaped obstacle. Therefore, except $\tilde{P}_{-r}$ and $\tilde{P}_{-1}$ assigned to adequate cells, two moderate-negative FPEs should locate at the vertices' cells of the cul-de-sac so that the created gradient directions not only point away from the cul-de-sac and then go towards the goal position, but also follow the shortest path. Which moderate-negative FPE located at which vertex's cells is based on a relative quantity compared with the FPEs at the previous and next cells in the planned path. Because the previous and next cell FPEs are $\tilde{P}_{-1}$ and $\tilde{P}_{-r}$, respectively, $\tilde{P}_{-2}$ is selected into the vertex cells so that the formed potential field flows forward $\tilde{P}_{-r}$'s position, the goal position. Fig. 16 shows their gradient trajectories due to miscellaneous initial positions. As shown in Fig. 16, regardless

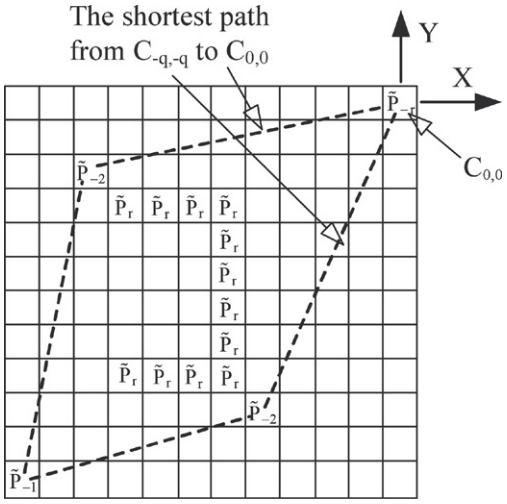

Fig. 15. The FPE layout for avoiding the cul-de-sac.

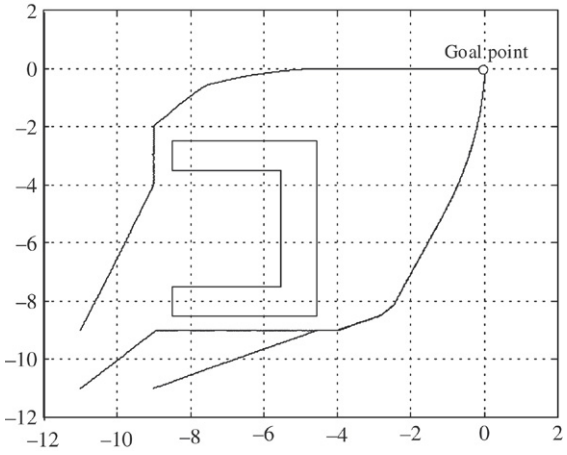

Fig. 16. The gradient trajectories due to different start positions.

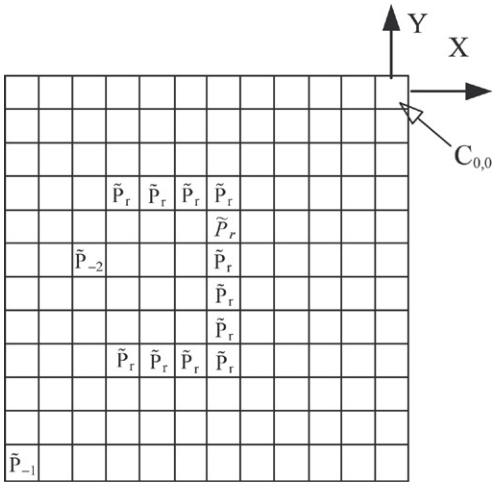

Fig. 17. The FPE layout for escaping the cul-de-sac.

of their initial position, the gradient trajectories go away from the obstacle and then arrive at the goal position.

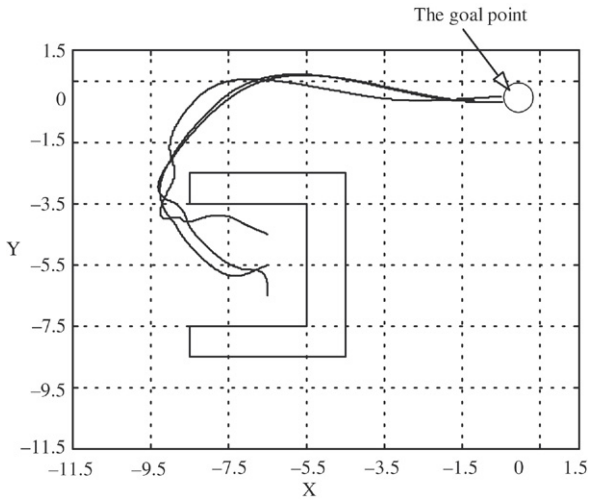

Fig. 18. The gradient trajectories for escaping the cul-de-sac and then for going towards the goal position.

Remark 6. The FPE map makes path planning strategy implemented for conducting a task easy. However how well the path is planned depends on how clear the knowledge possessed by an expert human is. In this case, assume that an expert human owns the knowledge to derive a visibility graph for a robot in a workspace. Then, the FPE map is built according to the visibility graph for avoiding dropping into the trap in a cul-de-sac, and for arriving at the goal position.

As inside, the mobile robot is dropping into the trap in the cul-de-sac. The navigation of general global path planning strategy should lead the mobile robot to first leave the trap and then to go towards the goal position. Because they result in the trap in the cul-de-sac, the negative FPEs $\tilde{P}_{-r}$ and $\tilde{P}_{-2}$ must be eliminated for neglecting the goal position and obstacle avoidance. After eliminating $\tilde{P}_{-r}$ and $\tilde{P}_{-2}$, as shown in Fig. 17, another $\tilde{P}_{-2}$ is assigned to the cell at the exit of the cul-de-sac for leaving the trap. After leaving the trap, i.e., arriving at the outside of the cul-de-sac, the FPE should navigate the mobile robot for obstacle avoidance and the goal point. Hence, the FPE layout is switched to Fig. 15 so that the mobile robot is navigated to stay away from the cul-de-sac and then go toward the goal point. Fig. 18 shows such gradient trajectories due to various initial positions from inside the cul-de-sac.

Remark 7. The FPE map makes navigation of the robot for conducting a sequence of tasks possible. In this case, a robot for conducting tasks switching between escaping the cul-de-sac trap and going towards the goal position is navigated by simply adjusting the FPE layout in the map.

Example 3. Navigation for a sequence of tasks.

The third example demonstrates that a sequence of tasks is navigated by assigning the FPE layout easily. In this example, there are two cases: one for avoiding the cul-de-sac through the door; and the other for that through the corridor. By placing FPEs at appropriate locations, the navigation paths produced

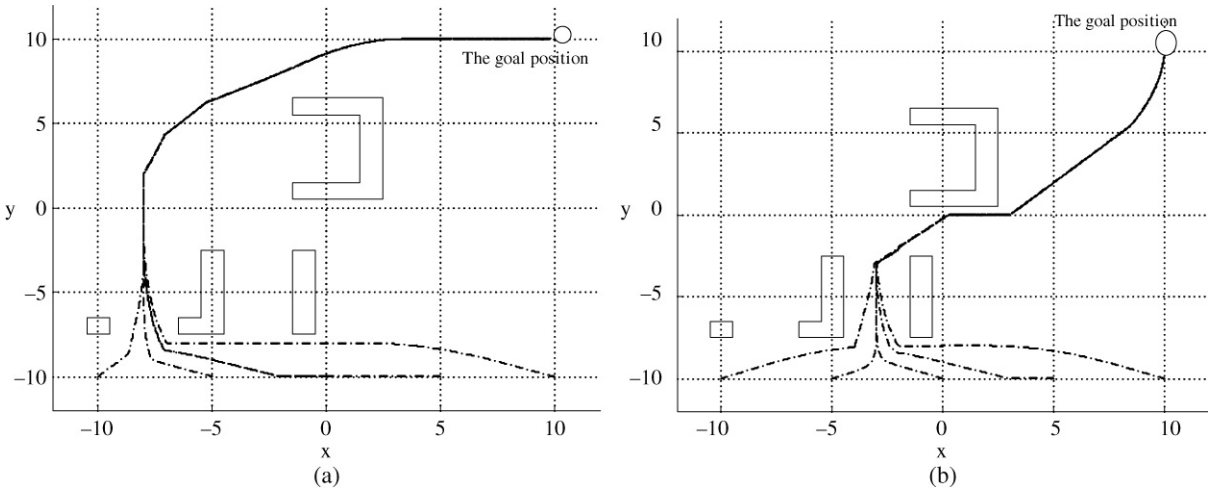

Fig. 19. Navigation paths going through the door or the corridor.

are shown in Fig. 19. Fig. 19(a) and (b) show navigation paths going through the door and through the corridor, respectively.

In summary, FPE assignment can according to the requirement of task navigation be based on qualitative information of a spatial model. There are two meaningful key points in FPE design. The first is that the FPE provides a way to make use of qualitative information for task navigation. The FPE navigation actually resulting in paths for conducting its tasks is the second of the key points. Such ideas are similar to Navigation templates including Substrate Navigation Templates (s-NaTs) and Modifier Navigation Templates (m-NaTs). The positive FPEs like M-NaTs are designed to avoid obstacles. One positive FPE pushes a mobile robot far away from an obstacle via eight directions, but m-NaTs via two directions, clockwise or counterclockwise. Unlike s-NaTs just guiding a task direction, many negative FPEs can be combined to guide a mobile robot following a complicated paths as shown in Fig. 19. In particular, expert knowledge such as visibility graphs can be implemented by FPEs for task navigation. This is the main advantage of the proposed FPE.

6. Conclusions and further development

In this paper, the FPE is proposed for building a special map that not only can form a potential field to navigate a mobile robot for a goal position like the potential field approach but can also utilize qualitative information for task navigating and conducting. Gradient trajectories of a built map are actual paths guiding a mobile robot to a goal position. The proposed FPE extends navigating from path to task.

It is easy for the proposed FPE to exchange tasks for a robot in different situations, for example a robot inside or outside a cul-de-sac. This is a way to solve a robot in inconstant situation for different tasks. In summary, the proposed FPE has the following advantages:

(1) The effective range of the FPE can be changed by adjusting the range of its membership function, e.g. the range of the most positive FPE $\tilde{P}_r$ only covers its neighborhood cells so that the resulting force repels mobile robots to stay away from the cells occupied by obstacles. In contrast, to attract mobile robots at any position in a workspace, the range of the most negative FPE $\tilde{P}_{-r}$ covers the entire workspace. The range of membership function solves the lack of local view of the potential field approach.

(2) The potential function formed by the FPE can be adjusted by replacing one cell's FPE. Compared to the potential field approach, the defined FPE is more flexible. In this paper, qualitative information such as the entrance and exit of a door, a corridor and a cul-de-sac and vertex points is engaged as the ground for locally adjusting potential distribution by negative FPEs.

(3) Via the FPE, the local path planning strategy can introduce the knowledge of a human expert for more sophisticated path planning strategy such as Example 2. In Example 2, visibility graphs usually based on expert knowledge are engaged to construct FPE maps for avoiding or escaping a cul-de-sac.

(4) It is easy for the FPE map to conduct robot navigation of a sequence of tasks illustrated in Example 3.

Based on the second type of fuzzy modeling, the FPE paves a way to convert qualitative information of a spatial model into metric information for task navigation. The map built by the FPE leads much human thinking injected into navigation such as navigation for a sequence of tasks illustrated in Example 3. In addition, just as imitating the visibility graph as depicted in Fig. 15, the FPE is able to combine many human requirements into task navigation. Task navigation that satisfies human requirements may be named intelligent navigation. This paper stimulates a further way to develop fuzzy modeling for intelligent navigation.

References

[1] Ta. Asano, Te. Asano, L.J. Guibas, J. Hershberger, H. Imai, Visibility of disjoint polygons, Algorithmica 1 (1) (1986) 49–63.

[2] O. Azouaoui, M. Ouaaz, A. Chohra, A. Farah, K. Achour, Fuzzy ArtMap neural network (FAMNN) based collision avoidance approach for autonomous robotic systems (ARS), in: 2001 Proceedings of the Second International Workshop on Robot Motion and Control, 2002, pp. 285–290.
[3] G. Beccari, S. Caselli, F. Zanichelli, Qualitative spatial representations from task-oriented perception and exploratory behaviors, Robotics and Autonomous Systems 25 (1998) 147–157.
[4] G. Borgefors, Distance transformations in arbitrary dimensions, Computer Vision, Graphics and Image Processing 27 (1984) 321–345.
[5] M. Braae, D.A. Rutherford, Theoretical and linguistic aspects of the fuzzy logic controller, Automatica 15 (5) (1979) 553–577.
[6] C.-L. Chen, P.-K. Chen, C.-K. Chen, Analysis and design of fuzzy control system, Fuzzy Sets and Systems 57 (1993) 125–140.
[7] D.Z. Chen, R.J. Szczerba, J.J. Uhran Jr., A framed-quadtree approach for determining Euclidean shortest paths in a 2-D environment, IEEE Transactions on Robotics and Automation 13 (5) (1997) 668–681.
[8] L.P. Chew, Planning the shortest path for a disc in $O(n \log N)$ time, in: Proc. ACM Symp. Computational Geometry, 1985, pp. 214–219.
[9] A. Chohra, A. Farah, M. Belloucif, Neuro-Fuzzy expert system E_S_CO_V for the obstacle avoidance of intelligent autonomous vehicle (IAV), in: Proceedings of the 1997 IEEE/RSJ International Conference on Intelligent Robots and Systems, vol. 3, 1997, pp. 1706–1713.
[10] E. Czogala, W. Pedrycz, Fuzzy rule generation for fuzzy control, Cybernetics and System 13 (3) (1982) 275–294.
[11] A. Elfes, Sonar-based real-world mapping and navigation, IEEE Transactions on Robotics and Automation 3 (3) (1987).
[12] L.P. Holmblod, J.J. Ostergaard, Control of a cement kiln by fuzzy logic, in: M.M. Gupta, E. Sanchez (Eds.), Fuzzy Information and Decision Processes, North-Holland, 1982, pp. 389–399.
[13] S. Kambhampati, L.S. Davis, Multiresolution path planning for mobile robots, IEEE Journal of Robotics and Automation RA-2 (3) (1986) 135–145.
[14] O. Khatib, Real-time obstacle avoidance for manipulators and mobile robots, The International Journal of Robotics Research 5 (1) (1986).
[15] J.B. Kiszka, M.E. Kochañska, D.S. Sliwiñska, The influence of some parameters on the accuracy of a fuzzy model, in: M. Sugeno (Ed.), Industrial Application of Fuzzy Control, North-Holland, 1985, pp. 187–230.
[16] B.J. Kuipers, Y.-T. Byun, A robust qualitative method for robot spatial learning, in: Proceedings of the Seventh National Conference on Artificial Intelligence, AAAI'88, August 1988, Saint Paul, MN, 1988.
[17] B.J. Kuipers, T.S. Levitt, Navigation and mapping in large-scale space, AI Magazine 9 (2) (1988).
[18] L.I. Larkin, A fuzzy logic controller for aircraft flight control, in: M. Sugeno (Ed.), Industrial Application of Fuzzy Control, North-Holland, 1985, pp. 87–103.
[19] D.T. Lee, R.L. Drysdale III, Generalized voronoi diagrams in the plane, SIAM Journal of Computing 10 (1) (1981) 73–87.
[20] Y.H. Liu, S. Arimoto, Finding shortest pah of a disc among polygonal obstacles using a radius-independent graph, IEEE Transactions on Robotics and Automation 11 (5) (1995) 682–691.
[21] Y.H. Liu, S. Arimoto, Path planning using tangent graph for mobile robots among polygonal and curved obstacles, International Journal of Robotics Research 11 (5) (1992) 376–382. MIT Press.
[22] Y.H. Liu, S. Arimoto, Proposal of tangent graph and extended tangent graph for path planning of mobile robots, in: Proc. IEEE Int. Conf. Robot. Automat., 1991, pp. 312–317.
[23] T. Lozano-Pérez, Spatial planning: a configuration space approach, IEEE Transactions on Computers 32 (2) (1983) 108–120.
[24] T. Lozano-Pérez, M.A. Wesley, An algorithm for planning collision-free paths among polyhegral obstacles, Communications of the ACM 22 (1979) 560–570.
[25] E.M. Mamdani, Application of fuzzy algorithms for control of a simple dynamic plant, Proceedings of the IEEE 121 (1974) 1585–1588.
[26] J. Mitchell, Shortest paths among obstacles in the plane, in: Proc. ACM symp. Computational Geometry, 1993, pp. 308–317.
[27] C. O'Dunlaing, C.K. Yap, A retraction method for planning the motion of a disc, Journal of Algorithms 6 (1985) 104–111.
[28] C. O'Dunlaing, M. Sharir, C.K. Yap, Retraction: A new approach to motion planning, in: Proc. 15th ACM Symp. On Theory of Computing, 1983, pp. 207–220.
[29] W. Pedrycz, Design of fuzzy control algorithms with the aid of fuzzy models, in: M. Sugeno (Ed.), Industrial Application of Fuzzy Control, North-Holland, 1985, pp. 153–173.
[30] H. Rohnert, Shortest paths in the plane with convex polygonal obstacles, Information Processing Letters 23 (1987) 71–76.
[31] T. Sasak, T. Akiyama, Traffic control process of express way by fuzzy logic, Fuzzy Sets and Systems 26 (2) (1988) 165–178.
[32] M.G. Slack, Navigation templates: Mediating qualitative guidance and quantitative control in mobile robot, IEEE Transactions on Systems Man and Cybernetics 23 (2) (1993) 452–466.
[33] M. Sugeno, M. Nishida, Fuzzy control of model car, Fuzzy Sets and Systems 16 (1985) 103–113.
[34] M. Sugeno, T. Takagi, A new approach to design of fuzzy controller, in: P.P. Wang, S.K. Chen (Eds.), Advance in Fuzzy Set, Possibility Theory, and Application, Plenum press, New York, 1983.
[35] M. Sugeno, K. Murakami, An experimental on fuzzy parking control using a model car, in: M. Sugeno (Ed.), Industrial Application of Fuzzy Control, North-Holland, 1985, pp. 125–138.
[36] T. Takagi, M. Sugeno, Fuzzy identification of systems and its application to modeling and control, IEEE Transactions on System Man and Cybernetics SMC-15 (1) (1985) 116–132.
[37] O. Takahashi, R.J. Schilling, Motion planning in a plane using generalized voronoi diagrams, IEEE Transactions on Robotics and Automation 6 (2) (1989) 143–150.
[38] K. Tanaka, M. Sugeno, Stability analysis and design of fuzzy control system, Fuzzy Sets and Systems 45 (2) (1992) 135–156.
[39] K. Tanaka, T. Ikeda, H.O. Wang, Robust stabilization of a class of uncertain nonlinear system via fuzzy control: Quadratic stabilizability, H_∞ control theory, and linear matrix inequalities, IEEE Transactions on Fuzzy Systems 4 (1) (1996) 1–13.
[40] N. Tomatis, I. Nourbakhsh, R. Siegwart, Hybrid simultaneous localization and map building: A natural integration of topological and metric, Robotics and Autonomous Systems 44 (2003) 3–14.
[41] K.I. Trovato, Differential {A*}: An Adaptive search method illustrated with robot path planning for moving obstacles and goals, and an uncertain environment, International Journal Pattern Recognition 4 (2) (1990) 245–268.
[42] R. Volpe, P. Khosla, Manipulator control with superquadric artificial potential functions: Theory and experiment, IEEE Transactions on System Man and Cybernetics 20 (6) (1990) 1423–1436.
[43] H.O. Wang, K. Tanaka, M.F. Griffin, An approach to fuzzy control of nonlinear systems: Stability and design issue, IEEE Transactions on Fuzzy Systems 4 (1) (1996) 14–23.
[44] E. Welzl, Constructing the visibility graph for n-line segments in $O(N^2)$ time, Information Processing Letters 20 (1985) 167–171.
[45] O. Yagishita, Application of fuzzy reasoning to the water purification process, in: M. Sugeno (Ed.), Industrial Application of Fuzzy Control, North-Holland, 1985, pp. 16–39.
[46] S. Yasunobu, S. Miyamoto, Automatic train operation system by predictive fuzzy control, in: M. Sugeno (Ed.), Industrial Application of Fuzzy Control, North-Holland, 1985, pp. 1–18.

Kuo-Yang Tu (M'98) was born in Tainan, Taiwan, ROC, in 1961. He received the B.S., M.S. and Ph.D. degrees in electrical engineering from National Taiwan University of Science and Technology, Taipei, Taiwan, in 1987, 1992 and 1998, respectively.

In 1998, he was appointed as Associate Professor with the Department of Electronic Engineering, HwaHsia College of Technology and Commerce. Currently, he is appointed as Associate Professor with the Institute of Systems and Control Engineering, National Kaohsiung First University of Science and

Technology. Since 1999, he has served concurrently as a patent screening member of the National Intellectual Property Office, Ministry of Economic Affair, Taipei, Taiwan, ROC. His current research interests and publications are in the area of intelligent computation, multi-agent system, system integration and Robotics. Specially, he had organized a team of robotics soccer for the competition of small-size league in EuRoboCup99 and RoboCup00 held on Amsterdam and Seattle, respectively.

Dr. Tu is a member of the IEEE Systems, Man, and Cybernetics Society, the IEEE Control Systems Society, the IEEE Computer Society, and the IEEE Robotics and Automation Society.

Jacky Baltes is an Associate Professor in the Department of Computer Science as well as the Department of Electrical and Computer Engineering at the University of Manitoba, and co-directs the Autonomous Agents Laboratory. He obtained his Ph.D. at the University of Calgary, and was previously a Senior Lecturer at the University of Auckland. His main research interests are robotics, computer vision, machine learning, and the application of these to complex problems, as well as the use of robotics in education.